



Research Article

Impact of Ultrasound-Assisted Dehydration on the Properties of Poly Lactic Acid Produced by Ring-Opening Polymerization

Nikmatuz Zahra¹, Endarto Yudo Wardhono², Hikmatun Ni'mah¹, Tri Widjaja^{1,*}

¹Department of Chemical Engineering, Faculty of Industrial Technology and Systems Engineering, Institut Teknologi Sepuluh Nopember, Surabaya, 60111, Indonesia

²Department of Chemical Engineering, Engineering Faculty, University of Sultan Ageng Tirtayasa, Cilegon, 42121, Indonesia

*Corresponding author: tri.widjaja@its.ac.id; Tel.: +62-31-5946240; Fax: +62-31-5999282

Abstract: The synthesis of polylactic acid (PLA) using Ring-Opening Polymerization (ROP) is composed of several stages, including pretreatment or dehydration, polycondensation, depolymerization, and polymerization. Dehydration is an important stage, which aims to remove the water content in lactic acid raw material. The water content can affect the polymerization and general properties of PLA formed. Therefore, this study aimed to maximize the dehydration process by using ultrasonic technology for lactic acid. The remaining water content was analyzed using Karl Fisher titration, while the final PLA product was assessed by Gel Permeation Chromatography (GPC), Differential Scanning Calorimetry (DSC), Fourier Transform Infrared (FTIR), and X-Ray Diffractometer (XRD). The results showed that the optimum conditions for ultrasonic dehydration optimized by Response Surface Methodology (RSM) were obtained at 98.85 minutes and a power rate of 109.60 watts with a moisture content of 1.9%. Subsequently, dehydrated lactic acid was polycondensed and depolymerized to form lactide. Ring-Opening Polymerization was carried out for 4 hours at 140°C, with the addition of a 0.2% w/w Stannous Octoate catalyst. The final result of PLA obtained by ultrasonic dehydration showed better characteristics than commercial products, with a crystallinity of 60.01%, and a melting temperature (TM) of 165.0°C. Additionally, the molecular weight obtained was 40,567 g/mol.

Keywords: Dehydration; Lactic acid; Response surface method; Ring-opening polymerization; Ultrasonic irradiation

1. Introduction

Poly(lactic acid) (PLA) is a thermoplastic monomer derived from renewable materials such as corn starch, sugar cane, and other natural resources (Lee and Hong, 2014). It is a well-known biodegradable aliphatic polyester made from lactic acid (LA), which has similar properties to polyethylene terephthalate, polyethylene (PE), polystyrene (PS), or polypropylene (PP) (Balla et al., 2021). Presently, PLA is one of the promising biomaterials with many applications in biomedical, packaging, automotive, and agriculture (Höhnemann et al., 2021; Reichert et al., 2020). It is a

This research was supported by the Ministry of Education, Culture, Research, and Technology (KEMENDIKBUD-RISTEK) of the Republic of Indonesia through the PMDSU Research Grant, contract number 1484/PKS/ITS/2022

<https://doi.org/10.14716/ijtech.v16i2.6521>

Received June 2023; Revised August 2023; Accepted August 2023

prospective material for addressing environmental issues due to the bio-compatible, biodegradable, and bio-based nature (Lololau et al., 2021; Nakajima et al., 2017).

Various processes, such as direct polycondensation, azeotropic polymerization, and ring-opening polymerization (ROP), generally synthesize PLA (Garlotta, 2019). Direct polycondensation is the most straightforward process, known as a one-step phase connecting monomers to form long chains accompanied by water removal. However, due to the difficulty in removing water byproducts, polymer produced by direct polycondensation is typically of low molecular weight and quality (Hu et al., 2016). This process needs severe conditions such as high temperature, low pressure, and long reaction times to achieve a high molecular weight (Maharana et al., 2009). In azeotropic polymerization, water is efficiently removed with a suitable azeotropic solution. The equilibrium between monomer and polymer is manipulated in an organic solvent to obtain a polymer with a higher molecular weight compared to condensation polymerization with a lower processing temperature. However, this method has limitations such as low yield, low purity, and solvent waste. ROP is a cyclic monomer propagation process that initiates an intermediate lactide by anionic or cationic insertion and regulates the chain-growth mechanism (Hu et al., 2016). Although the process has several stages, it can produce PLA with high molecular weight and purity (Kowalski et al., 2000). ROP is the most adopted method in PLA commercial production (Rahmayetty et al., 2018b).

In ROP route, LA is first dehydrated, followed by polycondensation to transform the acid into oligomers and further catalytically converted into lactide by cyclization depolymerization. The lactide ring then opens, forming high molecular weight PLA (de Albuquerque et al., 2021). LA dehydration stage is important in the synthesis of PLA, as the water content may trigger disturbances to polymerization and a decrease in product quality. Previous studies treated LA through conventional dehydration by heating at high temperatures and under vacuum pressure with a combination of nitrogen flow to eliminate water content (Jem and Tan, 2020). Sanglard et al. treated LA with a shallow pressure of 50 mbar and 120°C for 2 hours (Sanglard et al., 2012). Another study dehydrated LA with a temperature of 120°C and low-pressure conditions of 100 mbar (Horváth et al., 2021), while Nyiavuevang used a pressure of 60 kPa with heating for 2 hours (Nyiavuevang et al., 2022). These methods were carried out at longer processing times and with high energy consumption. Therefore, it is necessary to develop alternative energy such as ultrasonic to increase efficiency and reduce energy consumption in LA dehydration process (Dubey et al., 2017).

Ultrasonic radiation is an efficient method with many benefits, including time and cost efficiency, milder reaction conditions, and higher yields (Nagatomo et al., 2016). Therefore, this study aimed to examine the influence of ultrasonic pretreatment on the dehydration process in ROP route. Acoustic cavitation from ultrasonic waves can efficiently improve water loss with increased mass transfer and uniform heat distribution, thereby reducing energy consumption and increasing eco-friendly credentials. The optimum conditions, such as power rate and dehydration time, were optimized using Response Surface Method (RSM). The obtained PLA was tested by Fourier Transform Infra-Red Spectroscopy (FTIR) for chemical structure identification, including Proton Nuclear Magnetic Resonance Spectroscopy (HNMR), Gel permeation chromatography (GPC) for molecular weight, X-ray diffraction (XRD) for crystallinity index, and Differential Scanning Calorimetry (DSC) for thermal properties characterization. The physicochemical properties of the obtained product were then compared to the commercial type.

2. Methods

2.1. Materials

The materials used including LA (purity of 88-92% v/v), Chloroform, CHCl_3 (molecular weight, MW: 119.38 g/mol; density, ρ (25°C): 1.49 g/cm³), and Tin (II) Chloride Dihydrate, $\text{SnCl}_2 \cdot 2\text{H}_2\text{O}$ (MW: 225.63 g/mol, ρ (25°C): 2.71 g/cm³) were purchased from Merck, Darmstadt, Germany. Furthermore,

Stannous Octoate, $\text{Sn}(\text{Oct})_2$ (92.5-100% w/w; with MW: 405.12 g/mol), and Methanol, CH_3OH (98% v/v; ρ (25°C): 0.791 g/cm³) were obtained from Sigma Aldrich, Singapore. Nitrogen was supplied from Industrial Gas Samator, Mojokerto, Indonesia. All these materials and reagents were used without further purification.

2.2. Experimental Procedure

The experimental procedure in this study was divided into several stages, as shown in the schematic diagram in Figure 1.

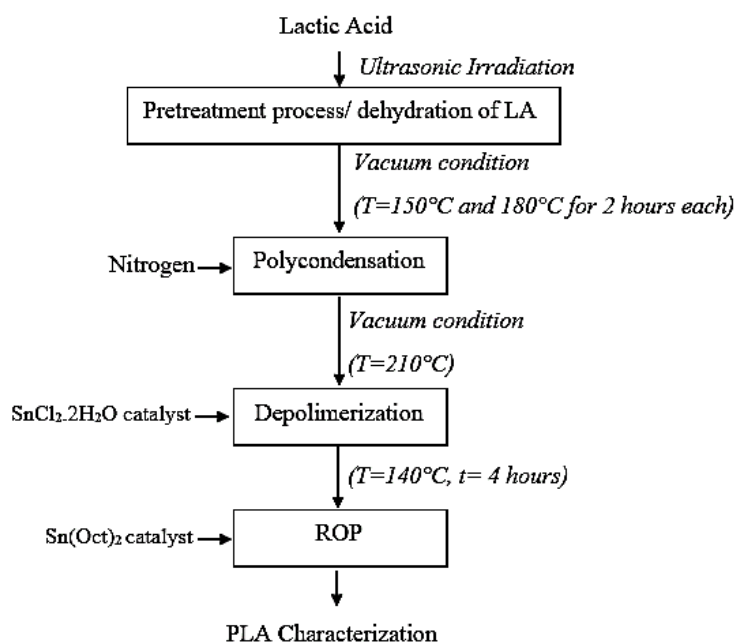


Figure 1 Schematic diagram of PLA synthesis method

2.2.1. Ultrasound-Assisted Dehydration

Lactic acid solution (50 mL) was placed into a 100 mL glass beaker and dehydrated using ultrasonic generator (Ultrasonic Cell Distrubtor UCD-P01, Biobase, Shandong, China) at 100°C. Ultrasound probe (5 mm diameter, 250 watts) was immersed into the solution with a fixed depth of 2 cm and a frequency of 20 - 30 kHz. The sonication time was varied at 30-120 min and the power rate at 30 - 180 watts. According to (Kestens et al., 2008), the water content of this solution was determined using Karl Fischer coulometer.

2.2.2. Polycondensation

The dehydrated lactic acid was placed in a 100 mL four-neck round-bottom flask fitted with a stir bar, thermometer, and condenser. The reaction was set at 150°C for 2 hours and then continued at 180°C for 2 hours (Rahmayetty et al., 2018b), during which nitrogen gas was flown to push out water vapor under vacuum pressure and 150 rpm of stirring.

2.2.3. Depolymerization

PLA oligomers produced from the polycondensation process were heated at 210°C under a vacuum and stirred at 150 rpm with the addition of 0.2% (w/w) catalyst. $\text{SnCl}_2 \cdot 2\text{H}_2\text{O}$ was selected as the catalyst at this stage in line with a previous study (Rahmayetty et al., 2015). The oligomer was heated until distillate was no longer produced. The vacuum valve was slowly closed after completing the process, then lactide was collected in a sample container and stored in a cooling chamber below 10°C.

2.2.4. Ring Opening Polymerization (ROP)

About 0.2% (w/w) of stannous octoate catalyst was added to the dried lactide, stirred at 150 rpm, and heated at 140°C for 4 hours. Subsequently, the obtained PLA was dissolved in chloroform, precipitated with methanol, filtered, and dried (Horváth et al., 2021).

2.3. Characterization

The total water content of LA was measured using Karl Fischer Moisture Titrator MKV-710S (Kyoto Electronics Manufacturing Co., Ltd., Kyoto, Japan). The functional groups of oligomers, lactide, and PLA products were determined using Nicolet iS10 FTIR spectrometer (Thermo Fisher Scientific, Madison, WI, USA). The scanning process was conducted on wavenumber 400-4000 cm^{-1} . Subsequently, the molecular structure of the samples was observed using NMR instrument JEOL ECS400 spectrometer (JEOL Ltd., Akishima, Tokyo, Japan) operated at 400 MHz (^1H) and 100 MHz (^{13}C). The molecular weight, M_w , and polydispersity index of the final PLA product were measured using GPC type HLC-8321GPC/HT (Tosoh Bioscience, Tokyo, Japan). The samples were eluted with chloroform at a flow rate of 0.3 mL/min and a column temperature of 40°C. The thermal characteristics were observed using DSC-60 Plus (Shimadzu, Kyoto, Japan). The samples were heated to 180°C, with a heating rate of 20°C/min under a nitrogen flow of 40 mL/min. Furthermore, X-ray diffraction patterns were recorded on a Philips X'pert PW3710 diffractometer. (PANalytical, Almelo, Netherlands). The samples were examined at a scanning angle of ($2\theta = 0-75^\circ$), a scanning rate of 1°/min using $\text{CuK}\alpha$ filtered radiation, 30 mA, 40 kV, and room temperature. Crystallinity index (CI) was calculated using Equation 1:

$$CI = \frac{A_c}{A_t} \times 100\% \quad (1)$$

where A_c represents crystalline curves' area and A_t is the total area of the curve.

3. Results and Discussion

3.1. Optimization of dehydration process

Pre-treatment or LA dehydration process is critical in synthesizing PLA, as it aims to eliminate the water content in the solution. Water content during polymerization is undesirable due to the ability to induce chain transfer, leading to the formation of PLA with a low molar mass (Khouri et al., 2022). During the polycondensation stage, water exists in equilibrium with LA, forming oligomers. Therefore, when water is not eliminated, the oligomer formation process will be hampered (Rahmayetty et al., 2018a). This study examined the use of RSM in Software Design Expert Version 13 to determine the optimal response of dehydration step by ultrasonic treatment. Central composite design (CCD) estimates the independent variables and interactions tested using ANOVA at a 95% confidence level (Esraa et al., 2022). The present experimental design is based on variables including time in minutes (X_1) and power rate in watts (X_2). Assuming the alpha (α) value is set at 1.41421, where α is the spacing of each axial point (star point) from the center point (Montgomery, 2020), the variables and levels are shown in Table 1.

Table 1 CCD matrix design of ultrasonic dehydration (with α value = 1.41421)

Independent Variables	Unit	Range and Level				
		-Alpha	-1	0	1	+Alpha
X_1 (Time)	Minutes	5.147	30	90	150	174.853
X_2 (Power Rate)	Watts	29.3	50	100	150	170.7

The experimental and predicted values obtained by response surface CCD are presented in Equation 2 as the second-order polynomial equation.

$$Y = b_0 + b_1X_1 + b_2X_2 + b_{11}X_1^2 + b_{22}X_2^2 + b_{12}X_1X_2 \quad (2)$$

Where Y is the percent of the water content, X_i is the control variable, b_i is the coefficient of the effect from X_i , and X_iX_j represents the interactions between the variables (Fegousse et al., 2019). CCD is composed of 2^n factorial, accentor, and $2n$ axial runs (Sadhukhan et al., 2016). Equation 3 was used to determine the number of experiments (N) as follows:

$$N = 2^n + 2n + f \quad (3)$$

Where n represents the number of control variables and f denotes the number of experiments carried out at the center point (Fegousse et al., 2019). Based on Equation 3, CCD experiment was carried out at 13 predetermined points, with repetition conducted at the midpoint ($X_1 = 0$ and $X_2 = 0$) five times. Response results of water content in LA solution (Y_1) are shown in Table 2.

The critical factors and the model efficiency were assessed by ANOVA according to the regression value and the mean square of the residual error (Chieng et al., 2012). As shown in Table 3, the criteria for a significant contribution of each variable are P-value < 5% and F-value > 5% (Harahap et al., 2019). The results confirmed that all factors had significant contributions to the model.

P-values for quadratic model were significant, with the coefficients being A (<0.0001), B (0.0240), AB (0.0004), A^2 (<0.0001), and B^2 (0.0088). The predetermined X_1 and X_2 points maximized the model, indicated by the smallest Y_1 response (% moisture content). The effect of experimental variables on the response was evaluated by examining the surface and contour plots, as shown in Figures 2a and 2b.

Table 2 Range and level of experiments on independent variables with CCD ($\alpha = 1.41421$)

Run	Variables		Experiment Results
	X_1 (min)	X_2 (watt)	Y_1 (% w/w)
1	90	170.7	2.46
2	30	150.0	3.41
3	90	100.0	2.14
4	90	100.0	1.89
5	174.853	100.0	4.27
6	150	50.0	2.92
7	90	100.0	1.97
8	90	100.0	1.93
9	90	29.3	2.89
10	90	100.0	2.32
11	150	150.0	3.66
12	5.147	100.0	6.2
13	30	50.0	5.15

Table 3 Analysis of variance (ANOVA) for quadratic model

Source	Sum of Squares	df	Mean Square	F-Value	P-Value	Significance
Model	21.38	5	4.28	108.99	< 0.0001	Significant
A-Time	2.77	1	2.77	70.67	< 0.0001	Significant
B-Power rate	0.3233	1	0.3233	8.24	0.0240	Significant
AB	1.54	1	1.54	39.20	0.0004	Significant
A^2	16.71	1	16.71	426.04	< 0.0001	Significant
B^2	0.5071	1	0.5071	12.93	0.0088	Significant
Residual	0.2746	7	0.0392			
Lack of Fit	0.1472	3	0.0491	1.54	0.3344	Not Significant
Pure Error	0.1274	4	0.0318			
Cor Total	21.65	12				

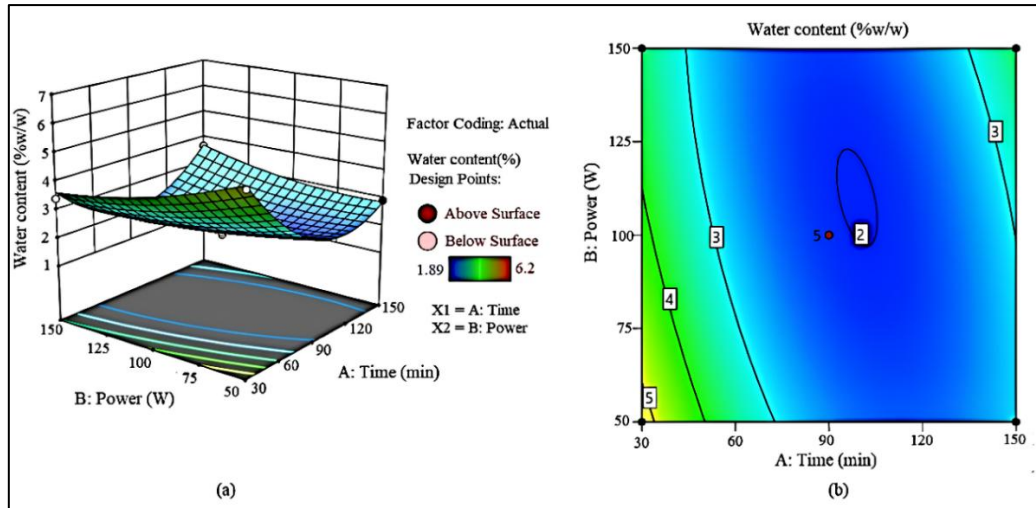


Figure 2 (a) Surface plot; (b) Contour plot of the optimization results

Based on Figure 2, response surface plot represents the value of the independent variable, which is on the horizontal axis perpendicular to the response. This plot showed a downward curved pattern, indicating that the lowest area was the optimum region (Hawashi et al., 2019). On the other hand, contour plots represent lines that show the response value (Y₁) of the minimum value up to the maximum. The empirical model that predicts the water content reduction as a function of time and power under optimal conditions is shown in Equation 4.

$$Y_1 = 9.76255 - 0.107978X_1 - 0.110551X_2 + 0.000431X_1^2 + 0.000675X_2^2 + 0.000517X_1X_2 \quad (4)$$

Table 4 Model summary of dehydration optimization

S	R-sq	R-Sq(adj)	R-sq(pred)
0.1981	98.73%	97.83%	94.25%

The coefficient of determination ($R^2 = 0.9873$) has a maximum value of 1, attained for a perfect fit (Zare-Dorabei et al., 2016). When R^2 value between experimental and prediction in regression is close to 1, this implies that the experimental information is appropriate and relative to the actual value. Furthermore, the difference between the sample values and the mean was measured using the standard deviation (S) (Andrade, 2020). At 0.1981, the S value found in this study was considered relatively low.

The desirability for optimization criteria described in Figure 3 showed that the optimum power for dehydration was 109.60 W at 98.85 minutes, with a water content of 1.99%. According to previous reports, the desirability value ranges from 0 - 1, representing maximum and minimum conditions, respectively.

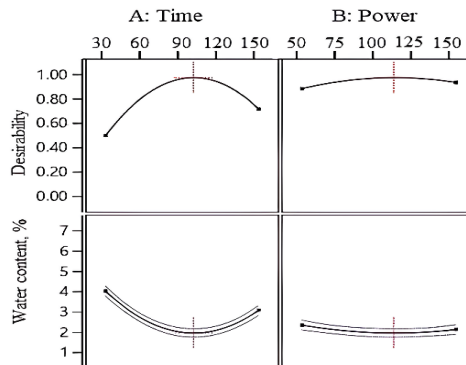


Figure 3 Desirability profile for time and power rate parameters

The data was retested to validate the optimum model by calculating an experimental error between theoretical and empirical values. The results obtained from the calculation are shown in Table 5.

Table 5 Validation of the optimum results

Time (min)	Power rate (W)	water content in lactic acid solution (%)			error
		I	II	average	
98.852	109.60	1.86	1.94	1.9	1.9858

The error acquired was below the limit (< 5%) for the repetition experiment, suggesting the optimum point was fit. Ultrasound-assisted dehydration was relatively effective for removing water in LA raw material. Table 6 compares the results of ultrasonic dehydration and conventional processes under identical conditions.

Table 6 Comparison of water content in LA after ultrasonic and conventional treatment

	Sample		
	Raw material	Ultrasonic treatment	Conventional dehydration
Water content, %	14.60	1.90	4.27

Based on the results, ultrasonic process proved better and more effective than the vacuum or conventional process in LA dehydration. Ultrasonic irradiation is an effective method for synthesizing organic products due to several benefits, including lower time and cost, lighter reaction conditions, as well as higher yield (Wardhono et al., 2021). The effectiveness of ultrasonics follows the theory of cavitation in the formation, development, and detonation of micron-sized waves that create high local energy (Nagatomo et al., 2016). When bubbles cavitate, localized hot spots form with temperatures and pressures exceeding 5000 K and 500 atm, respectively (Ibrahim and Shamsuddin, 2021). In addition, ultrasonic at low frequencies can affect physical processes, as well as improve mass transfer and emulsification (Nagatomo et al., 2016). The use of ultrasonics in LA dehydration process potentially increases mass transfer of water in the solution to the air, facilitating optimal water removal.

3.2. Polycondensation step

Polycondensation was carried out to produce an oligomer by subjecting LA solution to a glass reactor under a self-catalyzed reaction. The process was performed under nitrogen and vacuum conditions. The nitrogen line was used to reset atmospheric pressure and push out water vapor by-products to the condenser. The basic structure of produced oligomers was identified by FTIR and H-NMR, as shown in Figure 4.

FTIR spectra (Figure 4a) showed that oligomer LA (OLA) had carboxyl and hydroxyl groups. The carbonyl (C=O group) stretch of certain ester aliphatic appeared at 1748 cm^{-1} , suggesting the presence of a fat group (Wu et al., 2001). An absorption band centered at 1455 cm^{-1} was assigned to CH_3 asymmetric bending (Dovbeshko et al., 2000). C-H in-plane bending frequencies appeared at 1182, 1129, 1089, and 1043 cm^{-1} , while out-of-plane bending was observed at 871, 755, and 686 cm^{-1} , indicating characteristics of compound unsaturation. OLA is a shorter chain polymer, with slight differences from LA. The results are similar to those reported by Horvath (Horváth et al., 2021). The characteristic data for synthesized OLA are presented in Fig 4b. Based on H-NMR spectra, the peaks indicating a chemical shift (δ) were found at 1.44 - 1.47 ppm (CH_3 due to OH terminal of the 2-hydroxypropionate unit), 1.50 - 1.57 ppm (CH_3 for the lactate unit), 4.29 - 4.37 ppm (CH due to OH terminal of the 2-hydroxypropionate lactate unit), and 5.11 - 5.19 ppm (CH for lactate unit). The results show similarities with those reported by Rahmayetty (Rahmayetty et al., 2018b).

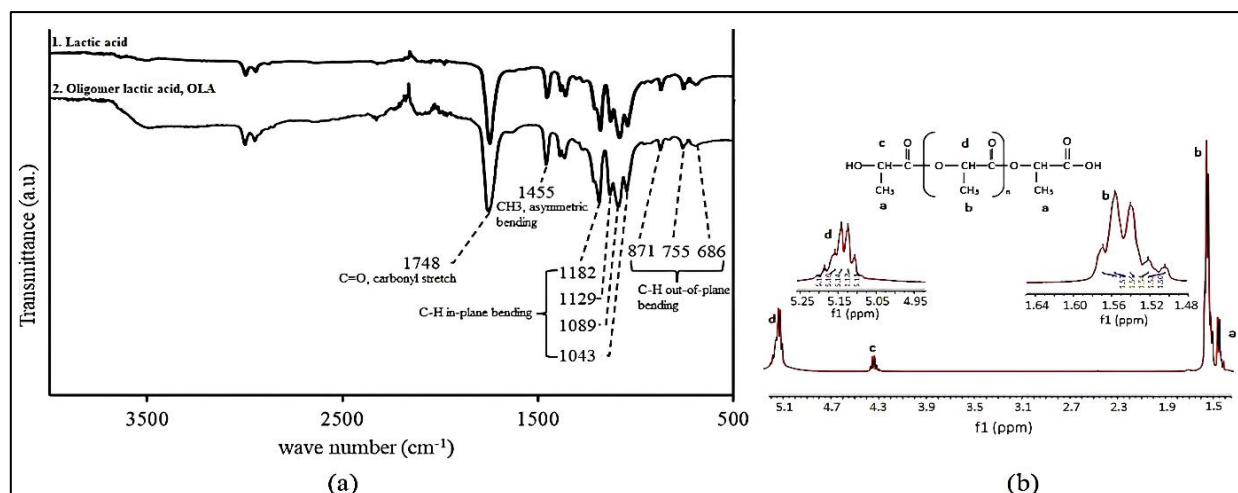


Figure 4 Characterization of OLA: (a) FTIR spectra; (b) H-NMR spectrum

3.3. Depolymerization step

In depolymerization step, oligomer was catalyzed to form the cyclic dimer of lactide. The reaction was conducted at a high-temperature vacuum to vaporize water and remove the product. Figure 5 shows FTIR and HNMR spectra of the cyclic dimer of lactide.

Figures 5a-1 and 5a-2 show IR absorption spectra of PLA sample from the commercial product and ROP step. Both samples had similar characteristics in which stretching frequencies for CH_3 symmetric, CH_3 asymmetric, $\text{C}=\text{O}$, and $\text{C}-\text{O}$ were observed at 1746, 2996, 2932, 1749, and 1099 cm^{-1} , respectively. Meanwhile, bending frequencies at 1445 and 1353 cm^{-1} were identified as asymmetric and symmetric CH_3 , respectively. The spectra obtained for lactide monomers are presented in Figure 5a-3. The absorption bands shown at 2996 and 2932 cm^{-1} as well as 1445 cm^{-1} represented symmetric and asymmetric stretch from CH_3 group, indicating that the methyl groups were present in the molecule (Nandiyanto et al., 2019). A high band at 1749 cm^{-1} was attributed to the carbonyl absorption of lactones $\text{C}=\text{O}$ (Herold et al., 2021), while the peak at 1267 cm^{-1} corresponded to $\text{C}-\text{O}-\text{C}$ bond from the lactonic ring. The band detected at 1080 cm^{-1} was assigned to symmetrical valence vibrations corresponding to $\text{C}-\text{O}-\text{C}$ linkage of the aliphatic chain, and the absorption peak at 930 cm^{-1} represented COO ring breathing mode (Muller et al., 2022). Figure 5b shows the chemical shift (δ) for depolymerized lactide, namely 1.53 - 1.56 ppm and 5.13 - 5.18 ppm. The first chemical shift signal is a doublet H which indicates the number of protons from CH group, a neighbor of the CH_3 group. Meanwhile, the second signal shows H quartet, which indicates the proton from CH_3 group, a neighbor of CH group. The results are similar to those reported by Rahmayetty (Rahmayetty et al., 2018b).

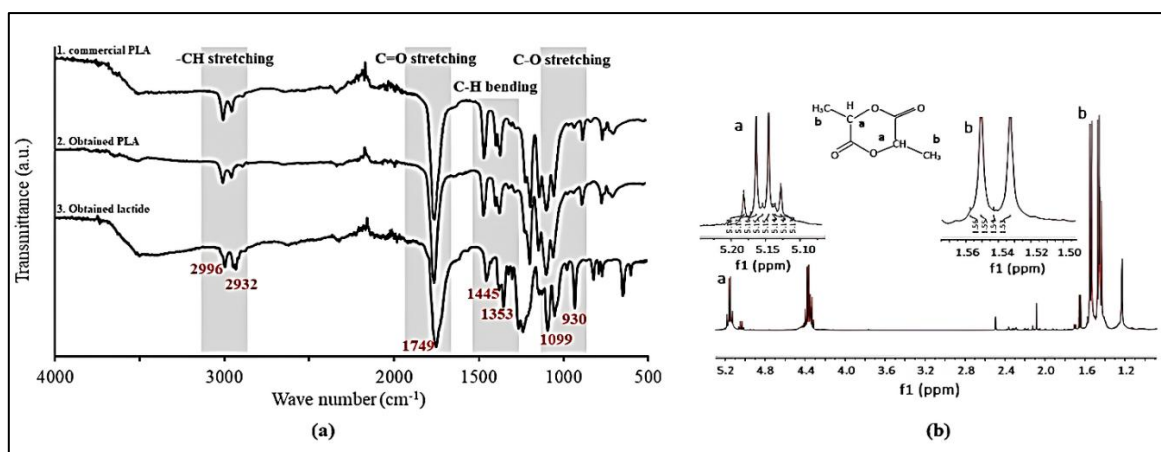


Figure 5 Characterization of samples; (a) FTIR spectrum; (b); H-NMR spectrum

3.4. Ring-opening polymerization

PLA polymerization through ROP method consists of two stages, namely initiation and propagation. During the initiation stage, coordination bonds form between the catalyst and lactide, leading to opening of the cyclic lactide and the formation of linear monomers. Meanwhile, during the propagation stage, chain elongation occurs (Budiyati et al., 2023). Alcoholic groups of hydroxyl compounds act as initiators in ROP of lactides, reacting with $\text{Sn}(\text{Oct})_2$ to generate a tin alkoxide bond by ligand exchange. Simultaneously, one of the carbonyl groups of lactide interacts temporarily with Sn atom. This coordination increases the nucleophilicity of the formed alkoxide and electrophilicity of lactide's carbonyl group, leading to the opening of lactide monomer. The alcoholic initiator becomes covalently bonded with the opened lactide and is subsequently deactivated. On the other side of the initiated monomer, a new hydroxyl formed can continue the initiation reactions of new lactide monomers and increase MW of PLA chains (Balla et al., 2021).

XRD profiles in Figure 6a showed two 2θ peaks in the synthesized PLA at 16.8° and 22.6° , corresponding to 101 and 002 crystallographic planes, respectively (He et al., 2008). Meanwhile, in commercial PLA, a shoulder broadening curve was observed from 11.5° to 18.1° indicating an amorphous region. Crystallinity index (CI) of synthesized PLA was 60.01%, relatively higher compared to the commercial type with a value of 38.80%. Polymers with higher CI are denser, leading to enhanced resistance. In addition, high crystallinity indicates an increase in the molecular weight of the polymer due to improved regularity of the structure (Teixeira et al., 2021). Lower water content in LA monomer enhances polymerization, leading to higher molecular weight and increased crystallinity.

Figure 6b shows a typical DSC thermogram of commercial PLA and the synthesized sample. Melting temperature (T_m) of commercial and synthesized PLA was 152.8°C and 165.0°C , respectively. The thermophysical properties were determined by molar mass, thermal history, and purity. Additionally, crystallinity of the polymer typically influences T_m . The low melting temperature was caused by the material's small and imperfect crystal size, lack of racemization, and impurities (Teixeira et al., 2021).

Table 7 shows data on the average molecular weight (M_w), average atomic number based on molecular weight (M_n), and Poly Dispersity Index (PDI). In general, PDI compares the average molecular weight (M_w) with atomic number (M_n). Based on the results, M_w and M_n of PLA with ultrasonic dehydration showed higher values than conventional dehydration, with a 59.87% increase in M_w . In contrast, PDI did not show a significant difference between the two values. Generally, this metric offers insights into the relationship between the water content of LA and molecular weight of PLA. The lower the water content, the better the polymerization process as indicated by the M_w results.

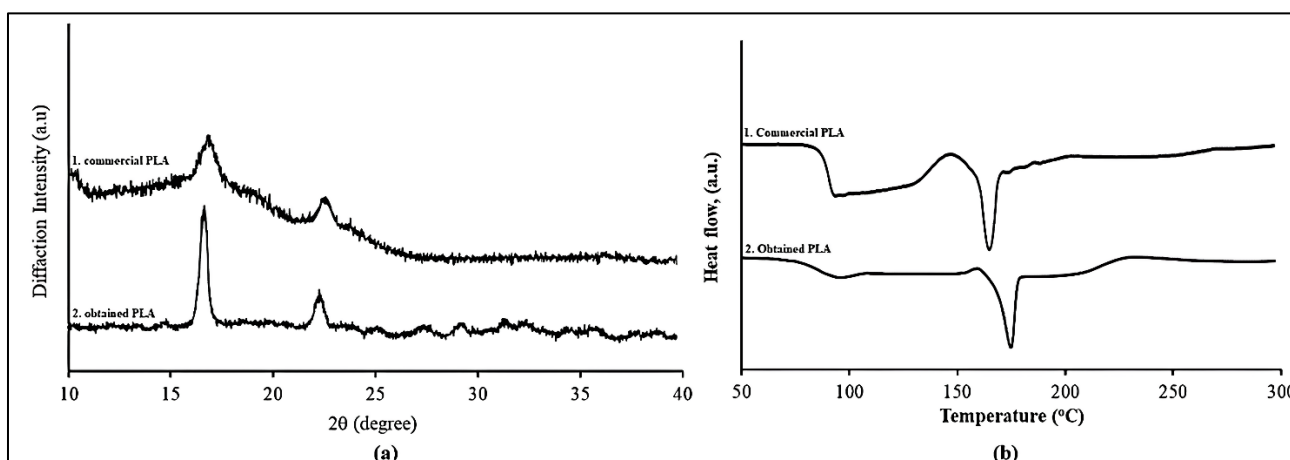


Figure 6 Characterization of PLA: (a) XRD pattern; (b) DSC thermogram

Table 7 Result of GPC analysis

Sample	Molecular Weight (Mw)	Molecular Number (Mn)	Poly Dispersity Index (PDI)
PLA with ultrasonic dehydration	40,567 g/mol	24,770	1.638
PLA with conventional dehydration	25,375 g/mol	15,802	1.606

Horvath reported that with initial dehydration for 1 hour, a temperature of 120°C, and a pressure of 100 mbar, the final Mw of PLLA was approximately 3,800 g/mol (Horváth et al., 2021). Meanwhile, Rahmayetty reported that by dehydrating LA for 1 hour at 100°C and continuously flowing nitrogen, the final product was PLA with Mw of 5,428 g/mol (Rahmayetty et al., 2018b). Based on the results of previous studies, dehydration with the assistance of ultrasonic irradiation can be superior and practical for producing higher molecular weight polymers. Ultrasonic pretreatment increases the concentration of monomers, leading to the formation of larger polymer particles than those produced by conventional polymerization (Nagatomo et al., 2016).

4. Conclusions

In conclusion, ultrasound-assisted dehydration of PLA synthesis using ROP method reduced the water content more effectively, while also improving the physical and thermal properties of the product. Optimization using RSM obtained the optimum conditions for ultrasonic dehydration at 98.85 minutes and a power rate of 109.60 watts with a moisture content of 1.9%. The final PLA product obtained by ultrasonic dehydration showed better characteristics than commercial type, with crystallinity of 60.01% and TM of 165.0°C. Additionally, the molecular weight was 40,567 g/mol. The use of ultrasonic irradiation in LA dehydration process is a potential method requiring further development in PLA synthesis with ROP.

Acknowledgements

The author is grateful to Indonesian Ministry of Education, Culture, Research, and Technology (KEMENDIKBUD-RISTEK) for the financial support with contract number 1484/PKS/ITS/2022. The author is also grateful to the Directorate of Research and Community Service of Institut Teknologi Sepuluh Nopember (DRPM-ITS) and Prof. Ir. Ali Altway, M.Sc., for the assistance in completing this study.

Author Contributions

N. Zahra: Investigation, Software, Formal Analysis, Writing – original draft. E.Y. Wardhono: Data curation, Supervision, Writing – review & editing, Validation. H. Ni'mah: Data curation, Supervision, Writing – review & editing, Validation. T. Widjaja: Conceptualization, Funding acquisition, Supervision, Validation.

Conflict of Interest

The authors declare no conflicts of interest.

References

- Andrade, C 2020, 'Understanding the difference between standard deviation and standard error of the mean, and knowing when to use which', *Indian Journal of Psychological Medicine*, vol. 42, no. 4, pp. 409-410, <https://doi.org/10.1177/02537176209334>
- Balla, E, Daniilidis, V, Karlioti, G, Kalamas, T, Stefanidou, M, Bikiaris, ND, Vlachopoulos, A, Koumentakou, I & Bikiaris, DN 2021, 'Poly (lactic acid): A versatile biobased polymer for the future with multifunctional properties - from monomer synthesis, polymerization techniques and molecular weight increase to PLA applications', *Polymers*, vol. 13, no. 11, p. 1882 <https://doi.org/10.3390/polym13111822>
- Budiyati, E, Rochmadi, Budiman, A & Budhijanto 2023, 'Hydroxylation kinetics of epoxidized tung oil using methanol as nucleophilic agent', *International Journal of Technology*, vol. 14, no. 5, pp. 1060-1071, <https://doi.org/10.14716/ijtech.v14i5.5376>

Chieng, BW, Ibrahim, NA & Yunus, WMZW 2012, 'Optimization of tensile strength of poly(lactic acid)/graphene nanocomposites using response surface methodology', *Polymer - Plastics Technology and Engineering*, vol. 51, no. 8, pp. 791-799, <https://doi.org/10.1080/03602559.2012.663043>

de Albuquerque, TL, Júnior, JEM, de Queiroz, LP, Ricardo, ADS & Rocha, MVP 2021, 'Polylactic acid production from biotechnological routes: A review', *International Journal of Biological Macromolecules*, vol. 186, pp. 933-951 <https://doi.org/10.1016/j.ijbiomac.2021.07.074>

Dovbeshko, GI, Gridina, NY, Kruglova, EB & Pashchuk, OP 2000, 'FTIR spectroscopy studies of nucleic acid damage', *Talanta*, vol. 53, no. 1, pp. 233-246, [https://doi.org/10.1016/S0039-9140\(00\)00462-8](https://doi.org/10.1016/S0039-9140(00)00462-8)

Dubey, SP, Abhyankar, HA, Marchante, V & Brighton, JL 2017, 'Microwave energy assisted synthesis of poly lactic acid via continuous reactive extrusion: Modelling of reaction kinetics', *RSC Advances*, vol. 7, no. 30, pp. 18529-18538, <https://doi.org/10.1039/C6RA26514F>

Esraa, A, Putra, A, Mosa, AI, Dan, RM & Attia, OH 2022, 'An empirical model for optimizing the sound absorption of single layer MPP based on response surface methodology', *International Journal of Technology*, vol. 13, no. 3, pp. 496-507, <https://doi.org/10.14716/ijtech.v13i3.5507>

Fegousse, A, El Gaidoumi, A, Miyah, Y, El Mountassir, R & Lahrichi, A 2019, 'Pineapple bark performance in dyes adsorption: Optimization by the central composite design', *Journal of Chemistry*, vol. 2019, pp. 1-11, <https://doi.org/10.1155/2019/3017163>

Garlotta, D 2019. 'A literature review of poly (lactic acid)', *Journal of Polymers and the Environment*, vol. 9, no. 2, pp. 63-84, <https://doi.org/10.1023/A:1020200822435>

Harahap, AFP, Rahman, AA, Sadrina, IN, Gozan, M 2019, 'Optimization of Pretreatment Conditions for Microwave-assisted Alkaline Delignification of Empty Fruit Bunch by Response Surface Methodology', *International Journal of Technology*, vol. 10, no. 8, pp. 1479-1487, <https://doi.org/10.14716/ijtech.v10i8.3431>

Hawashi, M, Aparamarta, H, Widjaja, T, Gunawan, S 2019, 'Optimization of Solid State Fermentation Conditions for Cyanide Content Reduction in Cassava Leaves using Response Surface Methodology', *International Journal of Technology*, vol. 10, no. 3, pp. 624-633, <https://doi.org/10.14716/ijtech.v10i3.2923>

He, J, Cui, S & Wang, SY 2008, 'Preparation and crystalline analysis of high-grade bamboo dissolving pulp for cellulose acetate', *Journal of Applied Polymer Science*, vol. 107, no. 2, pp. 1029-1038, <https://doi.org/10.1002/app.27061>

Herold, F, Leubner, O, Jeschonek, K, Hess, C, Drochner, A, Qi, W & Etzold, BJM 2021, 'Methodology for the identification of carbonyl absorption maxima of carbon surface oxides in DRIFT spectra', *Carbon Trends*, vol. 3, pp. 1-13, <https://doi.org/10.1016/j.cartre.2020.100020>

Höhnemann, T, Steinmann, M, Schindler, S, Hoss, M, König, S, Ota, A, Dauner, M & Buchmeiser, MR 2021, 'Poly(ethylene furanoate) along its life-cycle from a polycondensation approach to high-performance yarn and its recycle', *Materials*, vol. 14, no. 1044, pp. 1-15, <https://doi.org/10.3390/ma14041044>

Horváth, T, Marossy, K & Szabó, TJ 2021, 'Ring-opening polymerization and plasticization of poly(l-lactic acid) by adding of glycerol-diolate', *Journal of Thermal Analysis and Calorimetry*, vol. 147, no. 3, pp. 1-7 <https://doi.org/10.1007/s10973-020-10540-1>

Hu, Y, Daoud, WA, Cheuk, KKL & Lin, CSK 2016, 'Newly developed techniques on polycondensation, ring-opening polymerization and polymer modification: Focus on poly(lactic acid)', *Materials*, vol. 9, no. 133, pp. 1-14, <https://doi.org/10.3390/ma9030133>

Ibrahim, N & Shamsuddin, AN 2021, 'High molecular weight of polylactic acid (PLA): A review on the effect of initiator', *Malaysian Journal of Chemical Engineering and Technology*, vol. 4, no. 1, pp. 15-23, <https://doi.org/10.24191/mjcet.v4i1.12906>

Jem, KJ & Tan, B 2020, 'The development and challenges of poly(lactic acid) and poly(glycolic acid)', *Advanced Industrial and Engineering Polymer Research*, vol. 3, no. 2, pp. 60-70, <https://doi.org/10.1016/j.aiepr.2020.01.002>

Kestens, V, Conneely, P & Bernreuther, A 2008, 'Vaporisation coulometric Karl Fischer titration: A perfect tool for water content determination of difficult matrix reference materials', *Food Chemistry*, vol. 106, no. 4, pp. 1454-1459, <https://doi.org/10.1016/j.foodchem.2007.01.079>

Khouri, NG, Bahú, JO, Carvalho, BL, Wolf, R, Oswaldo, V, Concha, C & Maciel, R 2022, 'Lactic acid pre-treatment for lactide production - A techno-economic feasibility study for the dehydration step', *Chemical Engineering Transactions*, vol. 92, pp. 601-606, <https://doi.org/10.3303/CET2292101>

Kowalski, A, Libiszowski, J, Duda, A & Penczek, S 2000, 'Polymerization of L,L-dilactide initiated by tin(II) butoxide', *Macromolecules*, vol. 33, no. 6, pp. 1964-1971, <https://doi.org/10.1021/ma991751s>

Lee, C & Hong, S 2014, 'An overview of the synthesis and synthetic mechanism of poly(lactic acid)', *Modern Chemistry and Applications*, vol. 2, no. 4, pp. 1-5, <https://doi.org/10.4172/2329-6798.1000144>

Lololau, A, Soemardi, TP, Purnama, H & Polit, O 2021, 'Composite multiaxial mechanics: Laminate design optimization of taper-less wind turbine blades with ramie fiber-reinforced polylactic acid', *International Journal of Technology*, vol. 12, no. 6, pp. 1273-1287, <https://doi.org/10.14716/ijtech.v12i6.5199>

Maharana, T, Mohanty, B, Negi, YS 2009, 'Melt – solid polycondensation of lactic acid and its biodegradability', *Progress in Polymer Science*, vol. 34, pp. 99–124, <http://dx.doi.org/10.1016/j.progpolymsci.2008.10.001>

Montgomery, DC 2020, *Design and analysis of experiments*, 10th edn, John Wiley & Sons, Hoboken, NJ, USA

Muller, O, Hege, C, Guerchoux, M & Merlat, L 2022, 'Synthesis, characterization and nonlinear optical properties of polylactide and PMMA-based azophloxine nanocomposites for optical limiting applications', *Materials Science & Engineering B*, vol. 276, pp. 1-11, <https://doi.org/10.1016/j.mseb.2021.115524>

Nagatomo, D, Horie, T, Hongo, C & Ohmura, N 2016, 'Effect of ultrasonic pretreatment on emulsion polymerization of styrene', *Ultrasonics Sonochemistry*, vol. 31, pp. 337-341, <https://doi.org/10.1016/j.ultsonch.2016.01.010>

Nakajima, H, Dijkstra, P & Loos, K 2017, 'The recent developments in biobased polymers toward general and engineering applications: polymers that are upgraded from biodegradable polymers, analogous to petroleum-derived polymers, and newly developed', *Polymers*, vol. 9, no. 10, pp. 1-26, <http://dx.doi.org/10.3390/polym9100523>

Nandiyanto, ABD, Oktiani, R & Ragadhita, R 2019, 'How to read and interpret FTIR spectroscopy of organic material', *Indonesian Journal of Science & Technology*, vol. 4, no. 1, pp. 97-118, <https://doi.org/10.17509/ijost.v4i1.15806>

Nyaviuevang, B, Sodkampang, S, Dokmaikun, S, Thumanu, K, Boontawan, A & Junpirom, S 2022, 'Effect of temperature and time for the production of polylactic acid without initiator catalyst from lactide synthesized from ZnO powder catalyst', *Journal of Physics: Conference Series*, vol. 2175, no. 1, pp. 1-10, <https://doi.org/10.1088/1742-6596/2175/1/012042>

Rahmayetty, Sukirno & Gozan, M 2018a, 'Effect of polycondensation temperature to oligomer yield and depolymerisation side reaction', *World Chemical Engineering Journal*, vol. 2, no. 1, pp. 12-16

Rahmayetty, Sukirno, Prasetya, B & Gozan, M 2015, 'Effect of temperature and concentration of SnCl₂ on depolymerization process of L-lactide synthesis from L-lactic acid via short polycondensation', *International Journal of Applied Engineering Research*, vol. 10, no. 21, pp. 41942-41946

Rahmayetty, Whulanza, Y, Sukirno, Rahman, SF, Suyono, EA, Yohda, M & Gozan, M 2018b, 'Use of *Candida rugosa* lipase as a biocatalyst for L-lactide ring-opening polymerization and polylactic acid production', *Biocatalysis and Agricultural Biotechnology*, vol. 16, pp. 683-691, <https://doi.org/10.1016/j.bcab.2018.09.015>

Reichert, CL, Bugnicourt, E, Coltelli, M, Cinelli, P, Canesi, I, Braca, F, Alonso, R, Agostinis, L, Verstichel, S, Six, L, Mets, SD, Cantos, E, Ißbrücker, C, Geerinck, R, Nettleton, DF, Campos, I, Sauter, E, Pieczyk, P & Schmid, M 2020, 'Bio-based packaging: Materials, modifications, industrial applications and sustainability', *Polymers*, vol. 12, no. 7, pp. 1-35, <https://doi.org/10.3390/polym12071558>

Sadhukhan, B, Mondal, NK & Chattoraj, S 2016, 'Optimisation using central composite design (CCD) and the desirability function for sorption of methylene blue from aqueous solution onto *Lemna major*', *Karbala International Journal of Modern Science*, vol. 2, no. 3, pp. 145-155, <https://doi.org/10.1016/j.kijoms.2016.03.005>

Sanglard, P, Adamo, V, Bourgeois, JP, Chappuis, T & Vanoli, E 2012, 'Poly(lactic acid) Synthesis and Characterization', *Chimia*, vol. 66, no. 12, pp. 951-954, <https://doi.org/10.2533/chimia.2012.951>

Teixeira, S, Eblagon, KM, Miranda, F, Pereira, MFR & Figueiredo, JL 2021, 'Towards controlled degradation of poly(lactic) acid in technical applications', *Journal of Carbon Research*, vol. 7, no. 2, p. 42, <https://doi.org/10.3390/c7020042>

Wardhono, EY, Pinem, MP, Kustiningsih, I, Effendy, M, Clause, D, Saleh, K & Guénin, E 2021, 'Heterogeneous deacetylation reaction of chitin under low-frequency ultrasonic irradiation', *Carbohydrate Polymers*, vol. 267, p. 118180, <https://doi.org/10.1016/j.carbpol.2021.118180>

Wu, J, Xu, Y, Sun, C, Soloway, RD & Xu, D 2001, 'Distinguishing malignant from normal oral tissues using FTIR fiber-optic techniques', *Biopolymers*, vol. 62, no. 4, pp. 185-192, <https://doi.org/10.1002/bip.1013>

Zare-Dorabei, R, Jalalat, V & Tadjarodi, A 2016, 'Central composite design optimization of Ce(III) ion removal from aqueous solution using modified SBA-15 mesoporous silica', *New Journal of Chemistry*, vol. 40, no. 6, pp. 5128-5134, <https://doi.org/10.1039/C6NJ00239K>